Advanced Composite Materials
Publication details, including instructions for authors and subscription information:
http://www.tandfonline.com/loi/tacm20

Many aspects to improve the energy absorption capacity of collapsible energy absorber devices

E. Mahdi & A. S. M. Hamouda

Version of record first published: 02 Apr 2012.

To cite this article: E. Mahdi & A. S. M. Hamouda (2005): Many aspects to improve the energy absorption capacity of collapsible energy absorber devices, Advanced Composite Materials, 14:1, 1-23

To link to this article: http://dx.doi.org/10.1163/1568551053297085

Adv. Composite Mater., Vol. 14, No. 1, pp. 1–23 (2005)

Many aspects to improve the energy absorption capacity of collapsible energy absorber devices

E. MAHDI [1,*] and A. S. M. HAMOUDA [2]

[1] *Aerospace Engineering Department, Faculty of Engineering, University Putra Malaysia, 43400 UPM, Serdang, Selangor, Malaysia*
[2] *Mechanical and Manufacturing Engineering Department, Faculty of Engineering, University Putra Malaysia, 43400 UPM, Serdang, Selangor, Malaysia*

Received 7 November 2003; accepted 23 July 2004

Abstract—The behaviour of core and core-less composite elliptical thin-walled tubes subjected to quasi-static axial crushing is examined experimentally. The core-less tubes have two different arrangement systems (single and double). For the core tubes, natural cellular fibre was used as filler. Experiments showed that the crushing behaviours of the core-less tubes were found to be sensitive to their ellipticity ratio. Catastrophic failure mode is eradicated by both the arrangement system and the existence of the core, while the elastic energy is significantly suppressed by the existence of the core. The presence of core provides significant enhancement in tube damage tolerance and energy absorption per unit volume compared to the core-less tubes.

Keywords: Elliptical; core-less; composite; energy absorption; collapsible; natural cellular fibre; crushing.

NOMENCLATURE

A_1	Cross-section area of the material
A_2	Cross-section area of the structure
t	Thickness of the tube wall
a, b	Inner major and minor radii, respectively
a/b	Ellipticity ratio
P_m	Average crush failure load
P_i	Instantaneous crush failure load
E_m	Young's modulus of matrix
W_T	Total work done
s	Instantaneous deformation

*To whom correspondence should be addressed. E-mail: elsadig@eng.upm.edu.my

SE	Single core-less elliptical tube
SF	Single core elliptical tube
DE	Double elliptical tube
E_S	Specific energy absorbed
E_{NS}	Normalized specific energy absorbed
E_V	Volumetric energy absorbed
$\lfloor \boldsymbol{D}_{ij} \rfloor$	Bending stiffness matrix
$\lfloor \boldsymbol{A}_{ij} \rfloor$	Extension stiffness matrix
W_{picf}	Energy absorbed during the pre-initial-crush failure phase
W_{pcf}	Energy absorbed during the post-crush failure phase

Greek

ε	Densification strain
ρ	Mass density of the structure
σ_m	Average crush stress

1. INTRODUCTION

In the last three decades extensive and credible studies have proven the highly competitive ability of composite materials in the field of crashworthiness. It is also evident that structures composed of composite materials meet design requirements by the vehicle manufacturers as well as customers demand for a safe vehicle with low fuel consumption and high payload. It is also interesting to note that the relatively low cost glass/epoxy composite absorbs up to twice the specific energy of steel [1], while the relatively high cost carbon/PEEK composite can absorb up to seven times [2]. Therefore, it is expected that in the very near future more and more metals parts will be replaced by composite parts for weight saving and excellent reliability. However, the challenge is to find a suitably friendly polymeric composite material with specific features for a suitable structural application.

The high efficiency of any impact energy absorber device may be defined as its ability to decelerate smoothly the occupant compartment to rest within the allowable limit [3]. It is well-known that responses of axially crushed non-trigger tubes (i.e. tubes with constant thickness, straight wall and squared ends) are characterized by recording very high resistances values till they reach their full load-carrying capacity, after which definite different degrees of unstable behaviours take place [4].

However, due to the black and white design of any energy absorption device, one must define the desirable energy absorption device as one with suppressed energy absorption during the elastic or pre-initial crush failure stage. In such design and for gross deformation, the overall stability of the energy absorption device is important. Therefore, it is strongly believed that, for core-less tubular energy absorber devices, a stable load–deformation curve could be obtained only by steering the failure initiation to occur in a designed region along the shell meridional direction. In that manner, two approaches based on material and geometry properties have been suggested to avoid the Euler-buckling failure mechanism or any mechanism that leads to catastrophic failure, to suppress the elastic energy and to improve the crashworthiness parameters.

On one hand, approaches based on material properties are categorized into several groups. The first is to employ thin-walled structures with cores filled with crushable medium (i.e. synthesized or natural cellular material filler). Accordingly, it has been extensively shown that core tubes achieved high and stable load-carrying capacity along the gross deformation with high total energy and moderate specific energy absorption compared with the core-less tubes [5–8]. The second technique is to hybridize the tube wall layers using different fibres types [9]. The third method is to introduce a beneficial imperfection in the tube wall [10]. The fourth is also concerned with the tube wall: the author [11] has recently suggested segmented composite wall tubes in which three ranges of fibre reinforced/epoxy types were used including a stiff composite (carbon fabric fibre/epoxy), a relatively frangible composite material (a tissue mat glass fibre/epoxy) and highly compliant composite materials (cotton fabric fibre/epoxy).

On the other hand, approaches based on geometrical properties are also categorized in many groups. Accordingly, Farley [12] and Farley and Jones [13] reported that energy absorption capability is a non-linear function of inside diameter to wall thickness ratio (D/t) for tubular specimens. They stated that specific energy absorption was found to fall as D/t increased. Mamalis *et al.* [14] and Mahdi *et al.* [15] reported that the crushing behaviour is dominated by increase in the cone vertex angle.

There is comparatively little information available concerning the responses of core-less composite elliptical tubes to the quasi-static axial compressive load. But it would appear that no previous experimental or numerical studies have been made in the literature to study the crushing behaviour of composite elliptical tubes with core filled with natural cellular fibres. Treatment of this problem was restricted to metallic elliptical cross-section, carried out by Wu and Carney [16, 17]. They extensively investigated the collapse behaviour of braced elliptical tubes under lateral compressive load. They introduced their investigated structure to the field of crashworthiness as impact attenuation devices to be used in roadside safety application. Recently, researchers have started to address the problem of crushing behaviour of core-less composite elliptical tubes under quasi-static axial compressive load. Farely and Jones [13] studied the crushing characteristics of composite tubes with near-elliptical cross-section. Further, Meyres and Hyer [18] studied experimentally and semi-analytically the response of axially loaded composite elliptical tubes. Alkolose *et al.* [19] studied experimentally and numerically the response of axially loaded composite elliptical tubes. Studies on energy absorption capability as well as the load-carrying capacity of composite elliptical tubes are however still scarce. The primary aim of this study is to explore the ability of composite elliptical tubes as collapsible energy absorber devices.

2. EXPERIMENTAL

2.1. Geometry

We found that it is important to study the crushing behaviour of the tubes with elliptical cross-section, mainly because this might be due to their geometrical characteristics, in which they can occupy less space with reduced weight compared with other cross-sectional types, such as circular, rectangular, etc. Therefore, a number of composite tube specimens with elliptical cross-section were fabricated. All specimens were 150 mm high and 159.4 mm major diameter as shown in Fig. 1.

2.1.1. Core-less elliptical system. Woven, fabric or cloth composites present better energy management characteristics than the continuous or discontinuous filament composites. Woven roving glass fibre with orientation of [0/90] was selected to be the best candidate for fabricating the tube wall. This is because their intertwining fibre architecture prevents fibre micro-buckling failure mode as well as the gross delamination. Moreover, published energy absorption data revealed that circumferentially oriented fibres (90°) improved the energy absorption capability of composite structures. This is because they reduce the interlaminar cracks propagating between layers, which support the longitudinally oriented fibres (0°) to carry the applied load. This load resistance mechanism in turn could result in a large amount of energy dissipation compared with the filament fibres. The wet wrapping process was used to fabricate the specimen's wall. The average volume

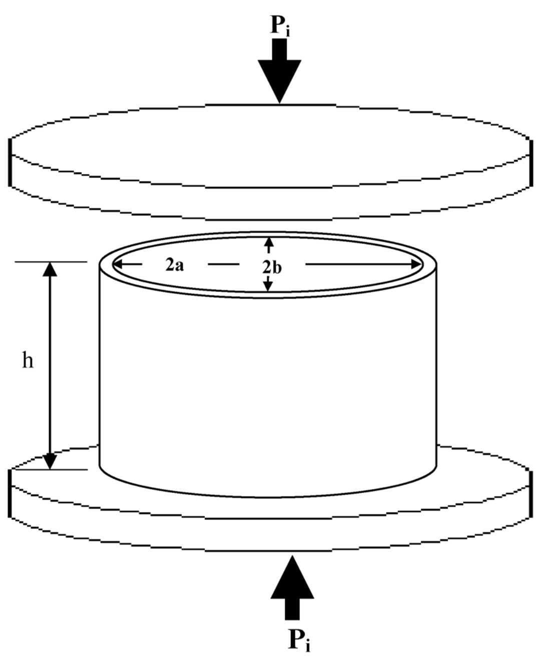

Figure 1. Notation of axial test of composite elliptical tube.

fraction used for the woven roving glass fibre was measured to be 0.55 ± 0.07%. More details about the fabrication process are also given in Ref. [19].

2.1.2. Cored single elliptical system. Engineering theory shows that the flexural stiffness $\lfloor \boldsymbol{D}_{ij} \rfloor$ of any structure is proportional to the cube of its thickness, $\boldsymbol{D}_{ij} = (1/3)(\sum Q_{ij}t^3)$. The purpose of a core is therefore to increase the laminate's bending stiffness by effectively thickening it with a low-density core material. This can provide a dramatic increase in bending stiffness for relatively little additional weight. Natural composite materials are increasingly being utilized in automotive parts, because of their relatively high strength and stiffness to weight and cost ratios. Available evidence indicates the advantage of using chopped natural fibre [20]. Therefore, chopped oil palm frond fibre mixed with resin in the form of foam was used as cores. The mass of filler required to obtain a desired density was poured into a tube, the ends of which were sealed to prevent the epoxy resin from flowing out. In consequence an average range of densities was obtained. A considerable effort was spent to make sure that filler densities were uniform over the inner volume of the tube. The stress–strain curve for chopped oil palm frond fibres mixed with resin is shown in Fig. 2. The work done per unit volume in crushing the natural cellular foam to a strain prior densification stage (ε) is simply the area under the stress strain curve. Very little energy is absorbed in the short, linear-elastic stage.

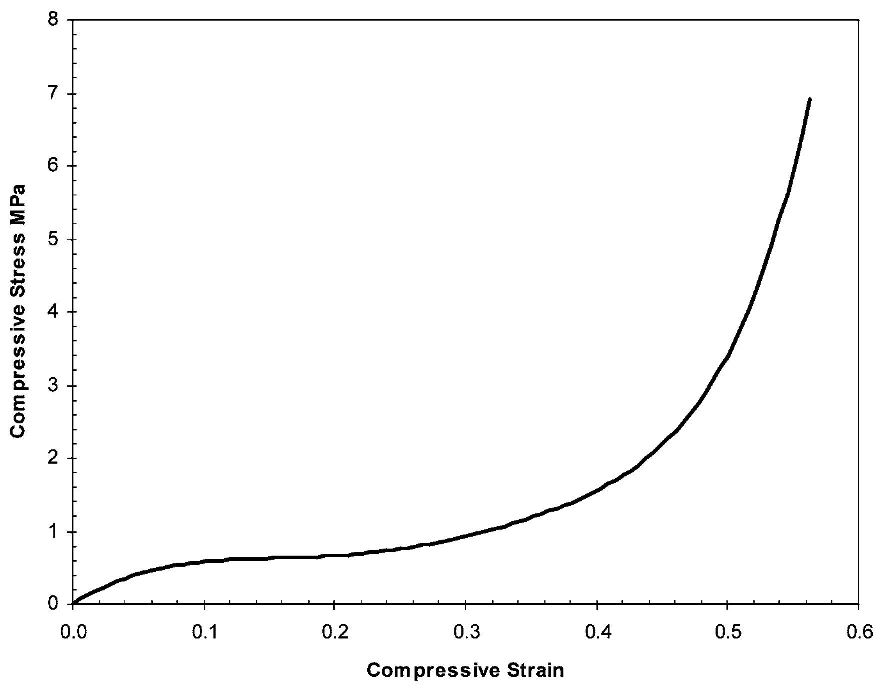

Figure 2. Compressive stress–strain curve for chopped oil palm frond fibres/epoxy.

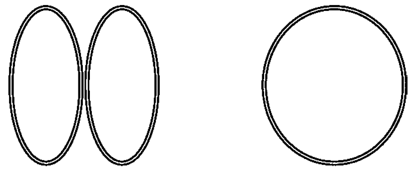

Figure 3. (a) Double elliptical tubes with ellipticity ratio of 2.00. (b) Single circular tubes.

As the figure shows, it is the long plateau of the stress–strain curve, arising from material crushing, that allows large energy absorption at almost constant load.

2.1.3. Core-less double elliptical tube system. Composite tube arrangement systems are proven to significantly influence the energy absorption capability of vehicles. Reid *et al.* [21] and Johnson and Reid [22] investigated the effect of tube arrangement on their energy absorption capability. In general, arrangement systems can be classified into two different types: loose packed (tubes arranged in a square array) or close packed. In this paper, loose packed arrangement is considered, in which only tubes with ellipticity ratio of 2 and equivalent densities of circular tube were fabricated for this test. This might be due to their geometric characteristics, in which they occupied space less than the space occupied by the circular tube as shown in Fig. 3.

2.2. Crushing test procedure

Reid [23] stated that when the tube is representative of a complete vehicle body shell, the dynamic loads are imposed at one end (the proximal end) while the other (distal) end is free. There is no quasi-static equivalent of such loading. Therefore, only a dynamic test is appropriate. This study concerns the use of a composite elliptical tube as a collapsible energy absorbing device within an automobile structure; the tube is supported at the distal end (i.e. point of attachment) by a stronger structure and is designed to behave in a manner similar to the quasi-static axial regular progressive mode. Therefore, quasi-static axial compression tests were performed on the tubes using an AMSLER-HB universal servo-hydraulic testing machine at a crosshead speed of 15 mm min^{-1}. Failure modes were investigated macroscopically using the photographs taken while the specimens were crushed. The photographs for all experiments were taken during the test; thus any photograph shows the specimen at some different crushing distance. The results obtained were taken as the average of at least three specimens for each case. The variation was $\pm 4\%$.

3. RESULTS AND DISCUSSION

Figures 4 to 20 illustrate the key results obtained from the quasi-static crushing tests. The crashworthiness parameters are expressed in terms of energy absorption

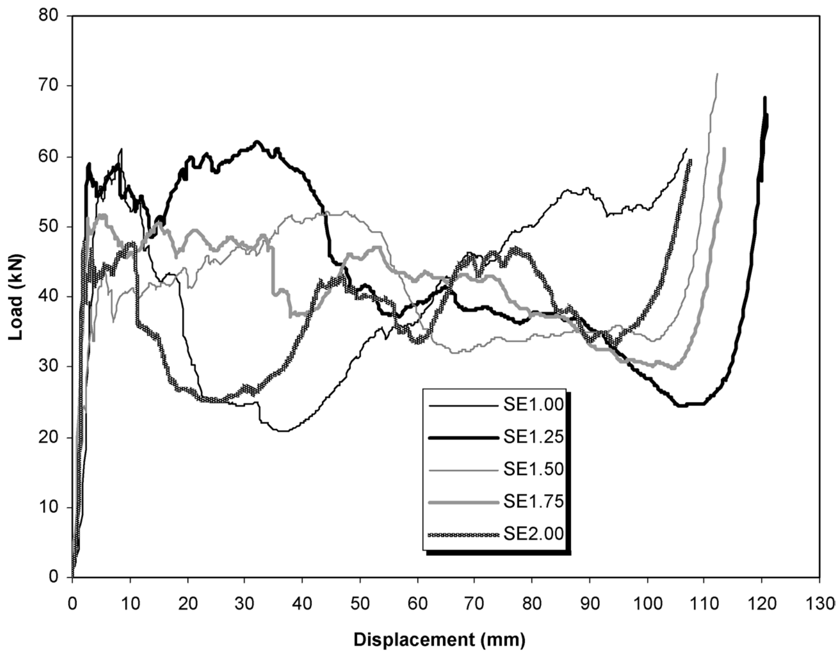

Figure 4. Load–deformation curves of single composite elliptical tubes with core-less.

Table 1.
Measured crashworthiness parameters

	P_m (MPa)	σ_m (MPa)	ε	E_{NS} (kJ/kg m^2)	E_V (MJ/m^3)	Mode of failure
SE1.00	40.24	50.63	0.72	10824.79	1.44	I
SE1.25	43.16	60.56	0.81	14973.93	2.17	I
SE1.50	40.51	61.63	0.69	15217.02	2.72	I
SE1.75	41.27	66.99	0.70	16318.50	3.12	II
SE2.00	37.09	63.04	0.66	22273.79	3.01	III
DE2.00	93.08	79.08	0.69	22273.79	4.45	III
SF1.50	207.51	17.61	0.53	862.12	9.58	IV
SF1.75	126.86	12.67	0.55	1302.69	11.43	IV
SF2.00	118.57	13.42	0.55	1190.47	10.60	IV

capabilities and load carrying capacity. Crashworthiness is defined as the energy absorbed per unit mass of material. The experimental data from the measured load–displacement responses are summarised in Table 1 in terms of mean crush failure load (P_m), normalized specific energy absorption (E_{NS}) and volumetric energy absorption (E_V).

3.1. Load–deformation curves

3.1.1. Core-less single elliptical tubes. The load–deformation curves for core-less tubes with different ellipticity ratios are shown in Fig. 4. It should be noted that the matrix material (epoxy) is not very weak compared to the fibre ($E_{\mathrm{m}} \succ 2$ GPa), so the matrix and the 90° oriented fibre prevent the 0° oriented fibre from local micro-buckling under small load. For the fibre oriented at 90° where the load is directed perpendicularly, most probably failure will be initiated at a stress level corresponding to the shear of the matrix. In this instant the load is characterized by inelastic and nonlinear behaviour until it reaches its first peak value. No stiffness reduction is considered due to matrix failure. This is because transverse matrix cracks alone usually do not have significant effect on the laminate stiffness. Following the first peak value, destruction of end faces caused by fibre debonding failure mode was observed. These micro-failure modes lead to loss of stability at the crushed zone and in turn lead to local surface ply separation (local delamination). This type of failure mode leads to bending stiffness degradation at the buckled zone, which results in different drop magnitudes of tube resistances depending on their ellipticity ratio. As the ellipticity ratio increases, the first drop magnitude as well as generally the load carrying capacity decreases. This is followed by a progressive local buckling or wrinkling mechanism with the first buckle forming away from the crushed end. These sequential deformations are repeated until the crushing load increases sharply. In this stage the structure behaves as a rigid body due to material densification phase. Three distinct initial failure-crushing modes were observed. These modes can be identified and classified as follows:

(i) Mode I. Multi-failure mode is a combination of progressive failure mode and local buckling mode, in which the crushing process was initiated by matrix crazing and cracking as shown in Figs 4, 5, 6, and 7. Consequently, after the first highest peak, progressive failure modes were developed from both ends accompanied by matrix fragmentation and transverse shearing as clearly seen in Figs 4–7. At this stage it is also observed that the main energy absorption mechanism is fracturing of lamina bundles or splaying mode. This stage is also characterized by stable load–deformation behaviour. Following the regular progressive failure mode, the tubes experience a change in crushing failure mode. They begin to crush in a local buckling at the mid-height of the tube. This change in crushing mode results in different drop magnitudes of tube load carrying capacity depending on their ellipticity ratio and as illustrated in Figs 4–7. The contribution of the mode to the total energy absorbed is smaller to that of the progressive failure mode. This observation was also observed by Farley [12] for glass/epoxy composite circular tubes. The energy absorbed by this type of failure mode is lower than those that fail by the pure regular progressive failure mode.

(ii) Mode II. This mode exhibits an initial progressive crushing mode followed by a drop-off in load carrying capacity observed in the immediate vicinity of the damaged region. The drop-off in load is larger than in mode I. In most cases a similar unstable crack forms, but it does not propagate around the whole circumference and therefore causes only a slight drop in load. The load recovers to

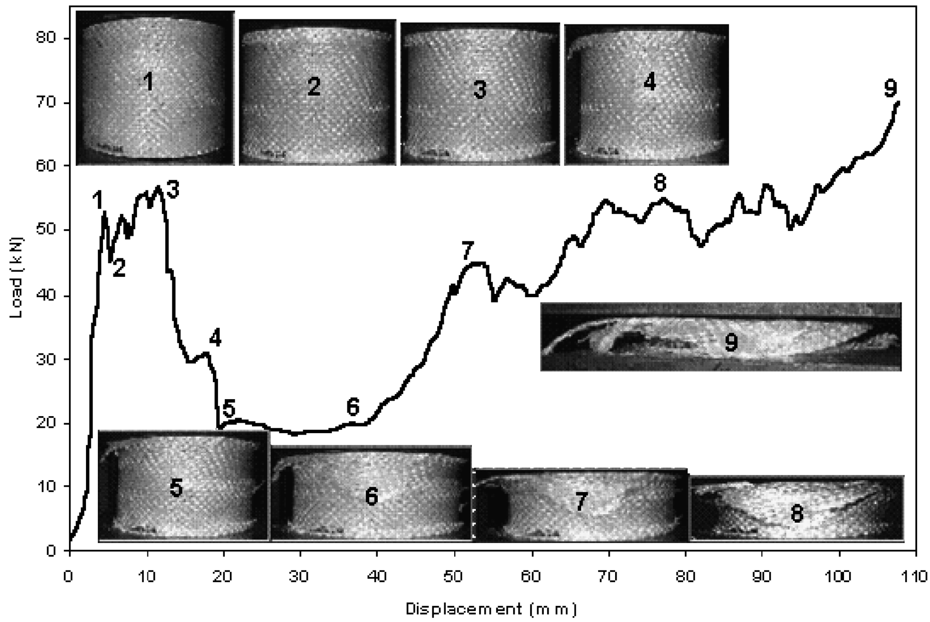

Figure 5. Typical load–deformation history of axially loaded single composite elliptical tube with core-less and a/b ratio of 1.00.

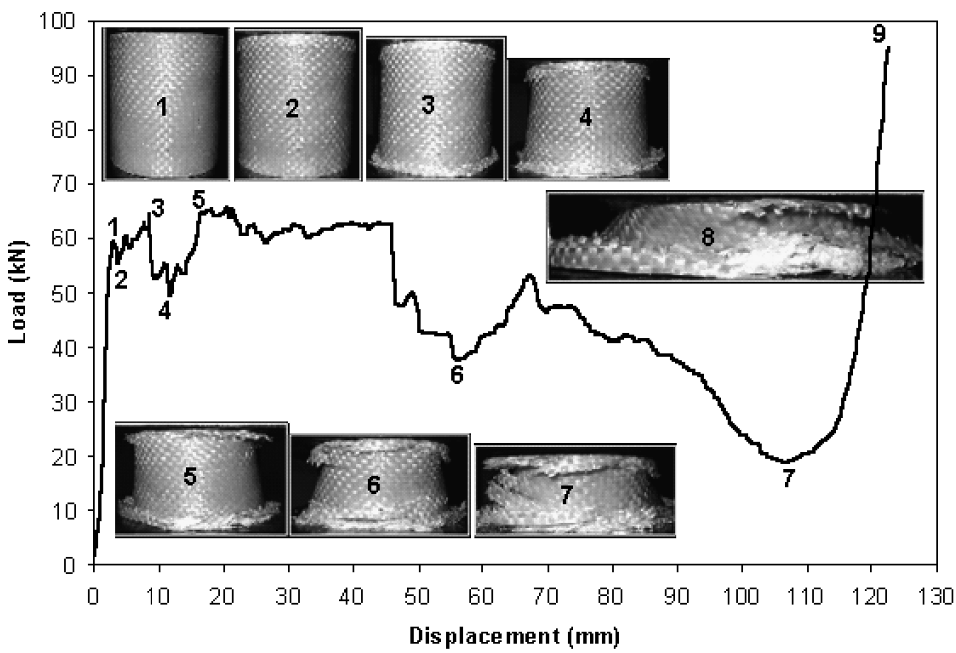

Figure 6. Typical load–deformation history of axially loaded single composite elliptical tube with core-less and a/b ratio of 1.25.

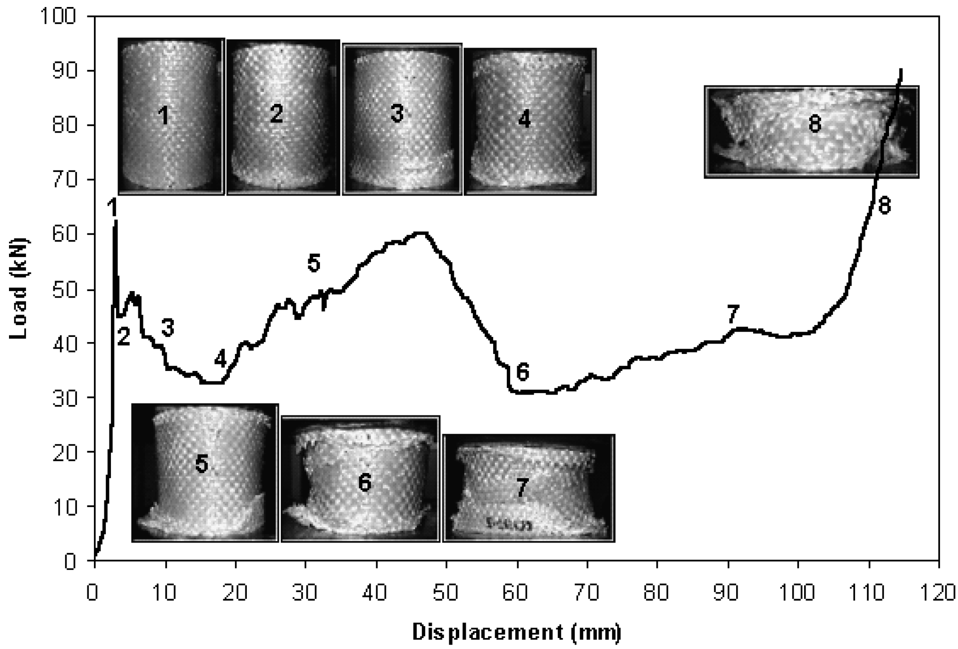

Figure 7. Typical load–deformation history of axially loaded single composite elliptical tube with core-less and a/b ratio of 1.50.

the steady state level after the crush zone passes through the damage area as clearly seen in Fig. 8 point 5.

(iii) Mode III. Pure regular progressive mode occurring from one end dominates the crushing process of axially crushed composite elliptical tubes with ellipticity ratio of 2.00. This mode is associated with a crush mechanism that involves extensive matrix deformation and fibre micro-fracture in small zones that moves progressively through the structure (see Fig. 9). The load–deformation behaviour of this type of failure is shown to be very stable along the post crush stage. Further, it is also evident from Table 1 that this type of progressive failure mode exhibited highest normalized specific energy absorption.

3.1.2. Cored single elliptical tubes. To explore the responses of cored elliptical tubes, natural fibre filled elliptical woven roving elliptical tubes were tested under quasi-static axial loading conditions. Ranges of ellipticity ratios were examined and the results are presented. Figure 10 presents average load–displacement curves for cored single elliptical tubes. It is evident that, as the crushing process progresses, the natural fibre filler in the crushed region gets stiffer due to a densification phase process, which in turn controls the deformation of the first zone to the initiation of other crushed zone. The filled tubes deformed in a similar manner but it was observed that the cored tube with ellipticity ratio of 1.50 (Fig. 11) showed the formation of an observable local ply separation at top end face during the pre-crush

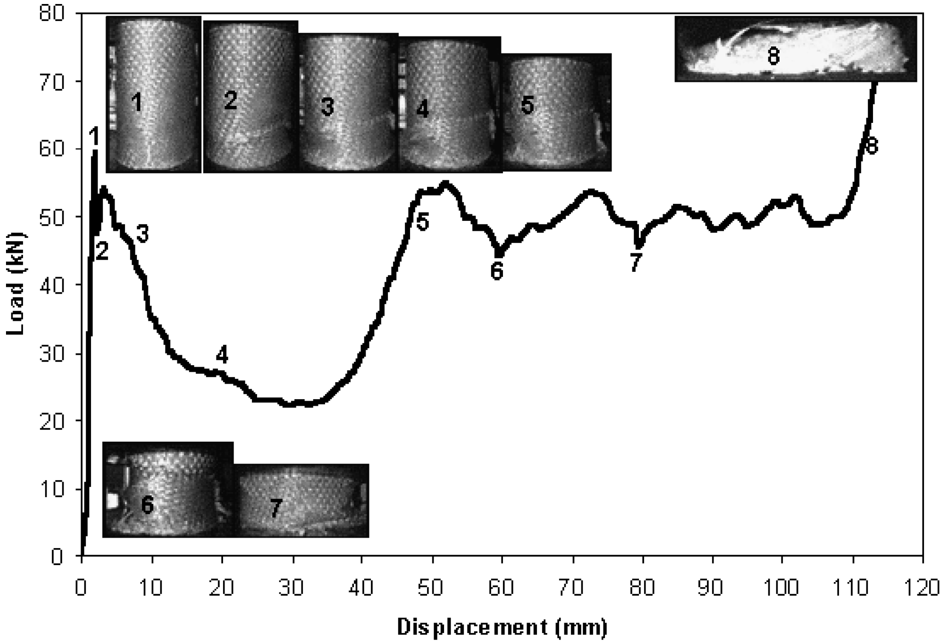

Figure 8. Typical load–deformation history of axially loaded single composite elliptical tube with core-less and a/b ratio of 1.75.

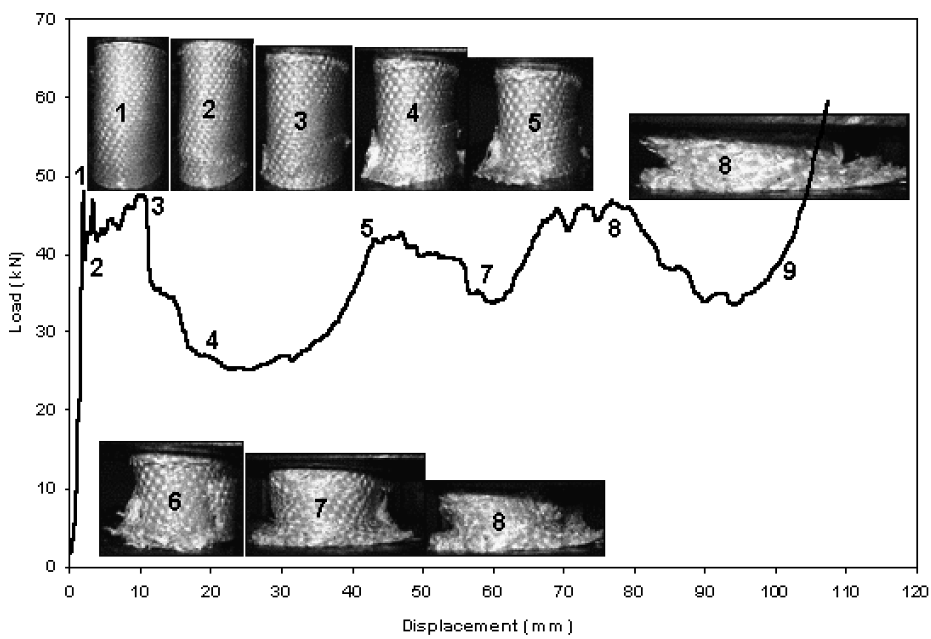

Figure 9. Typical load–deformation history of axially loaded single composite elliptical tube with core-less and a/b ratio of 2.00.

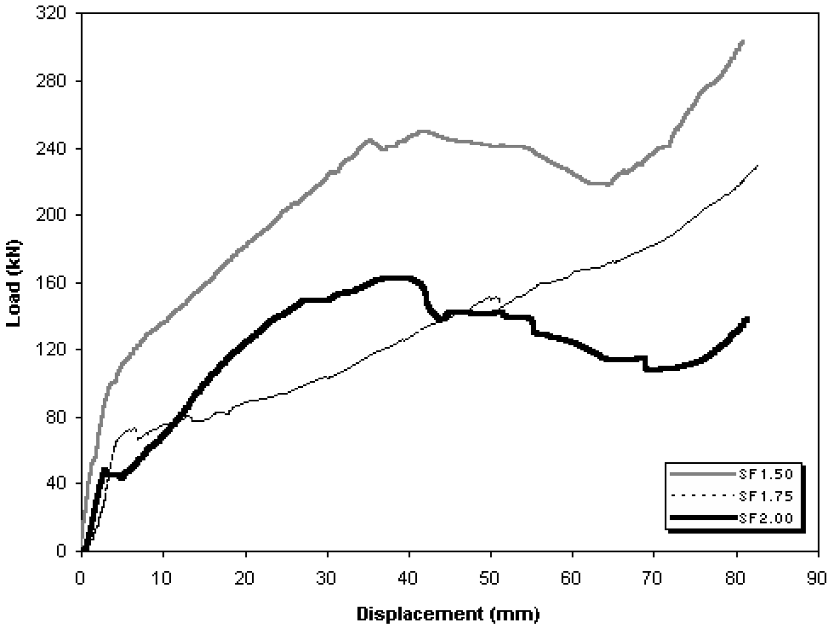

Figure 10. Load–deformation curves of single composite elliptical tubes with core.

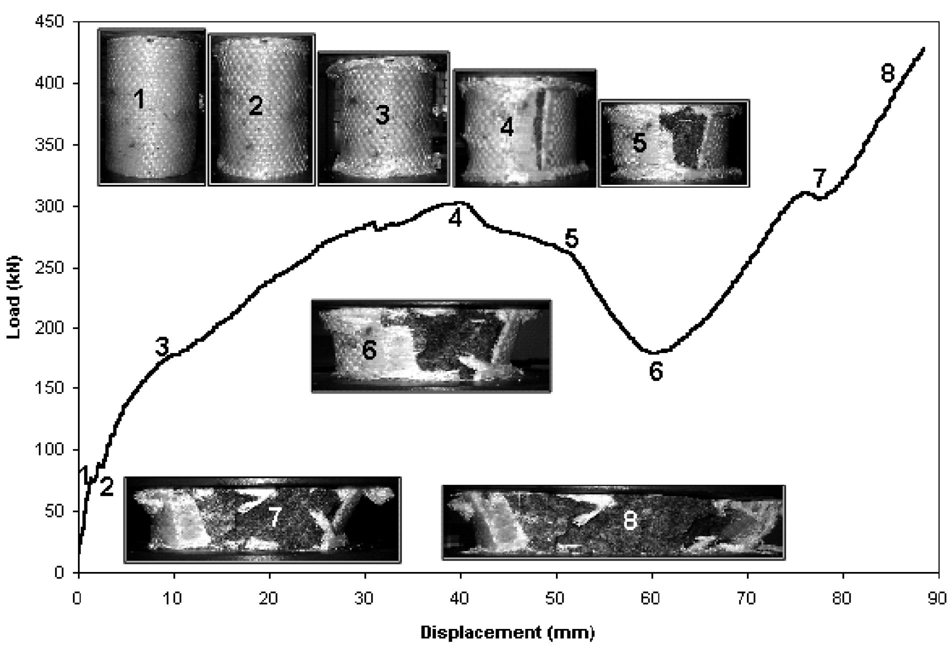

Figure 11. Typical load–deformation history of axially loaded single composite elliptical tube with core and a/b ratio of 1.50.

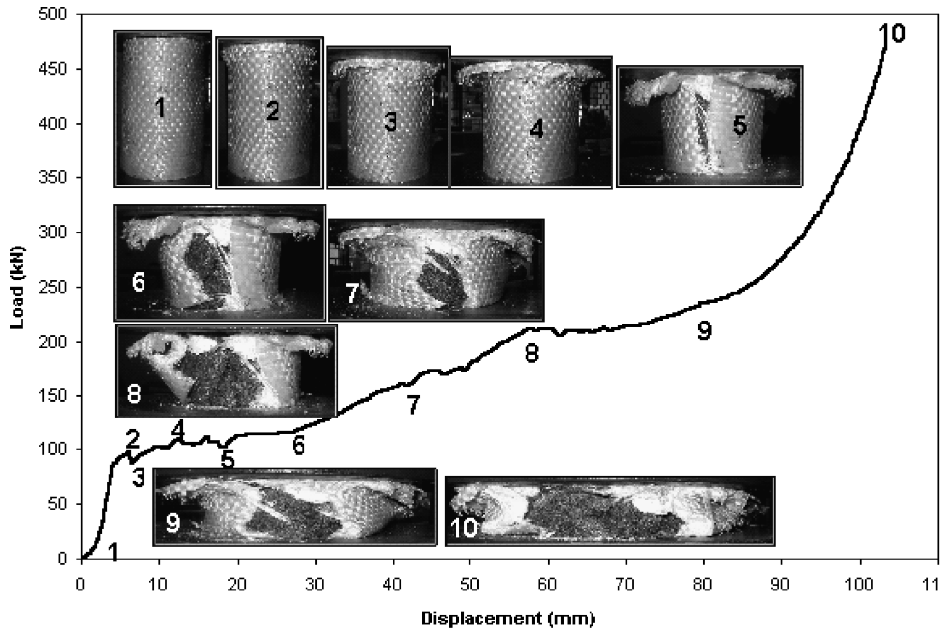

Figure 12. Typical load–deformation history of axially loaded single composite elliptical tube with core and a/b ratio of 1.75.

failure stage in contrast to the other cases, where destruction of end faces dominate the pre-crush failure stages, as clearly shown in Figs 12 and 13. In general, it is seen that, as the circumferential deformation of wall tube at the crushed zone increases, the filler in this crushed zone gets stiffer due to material densification. This arrests the axial as well as circumferential deformation of this zone leading to the initiation of out-plane tearing failure mode (Mode IV) as also clearly shown in Figs 11–13. The tearing mode fractured the 90° oriented fibres by fibre pull-out mode and is believed to be initiated by tensile hoop stress that results from the core expansion in circumferential direction. Growth of the thoroughly longitudinal crack dominates the post-crush failure stage of the tubes with cores. The presence of core also prevents the inward deformation of the tube wall during the crushing process in contrast with core-less tubes. On the other hand the core-tubes have lower stroke efficiency compared with the core-less tubes.

3.1.3. Core-less double elliptical tubes. Figure 14 shows a typical load–displacement curve for core-less double elliptical tubes crushed by a moving flat platen. It is seen that the double system initially goes through elastic deformation as shown in the range (1–2) in Fig. 12. Then the inelastic deformation occurs as seen in range (2–3). At this instant the system crush progressively while maintaining sustained crushing load value of 105 kN. The system was also achieving high stroke efficiency (~80% of the initial height) while maintaining sustained crushing load value of 105 kN. The system also showed high post-crash integrity in which the

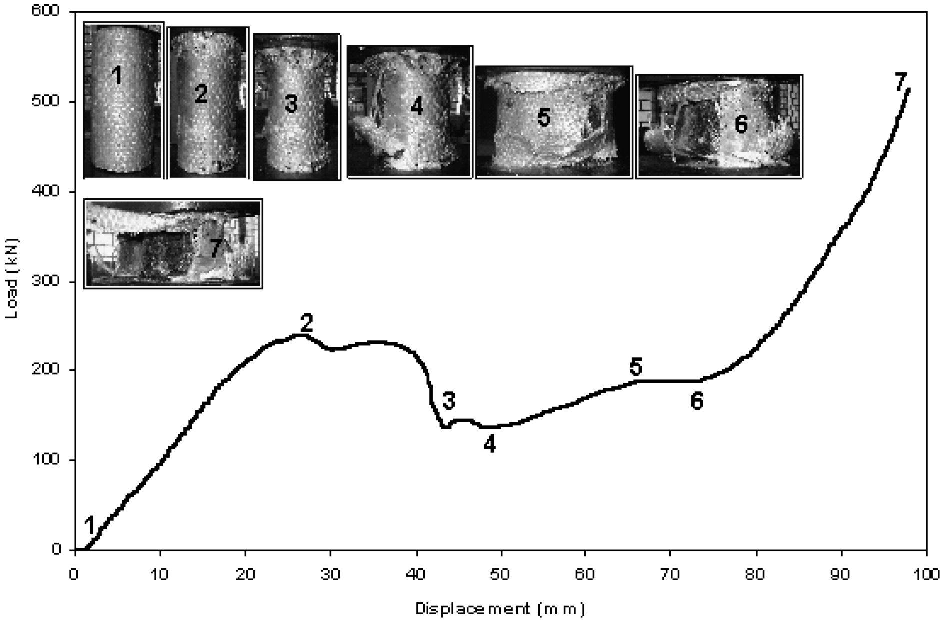

Figure 13. Typical load–deformation history of axially loaded single composite elliptical tube with core and a/b ratio of 2.00.

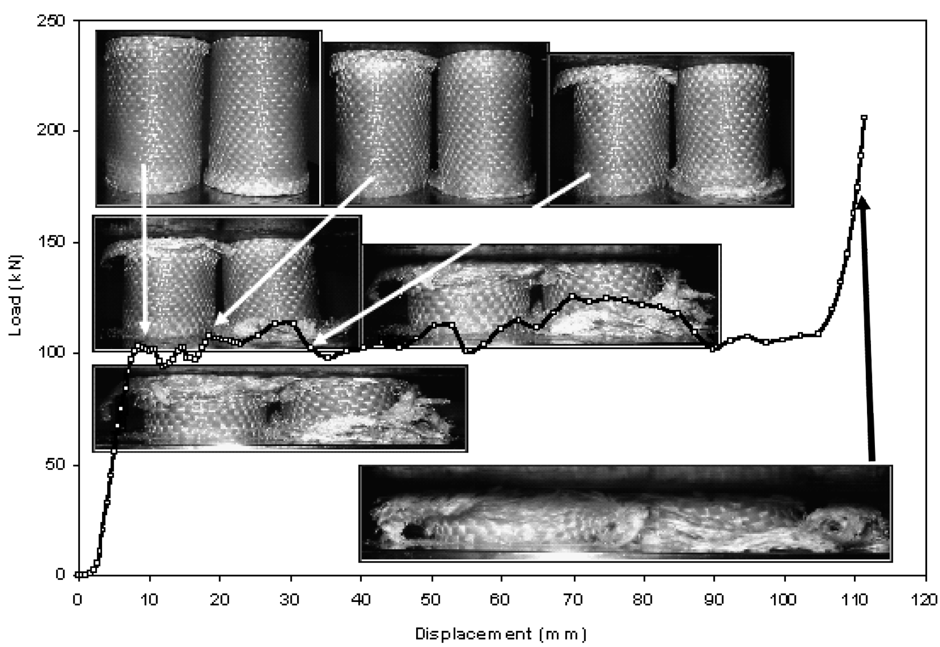

Figure 14. Typical load–deformation history of axially loaded double composite elliptical tube with core-less and a/b ratio of 2.00.

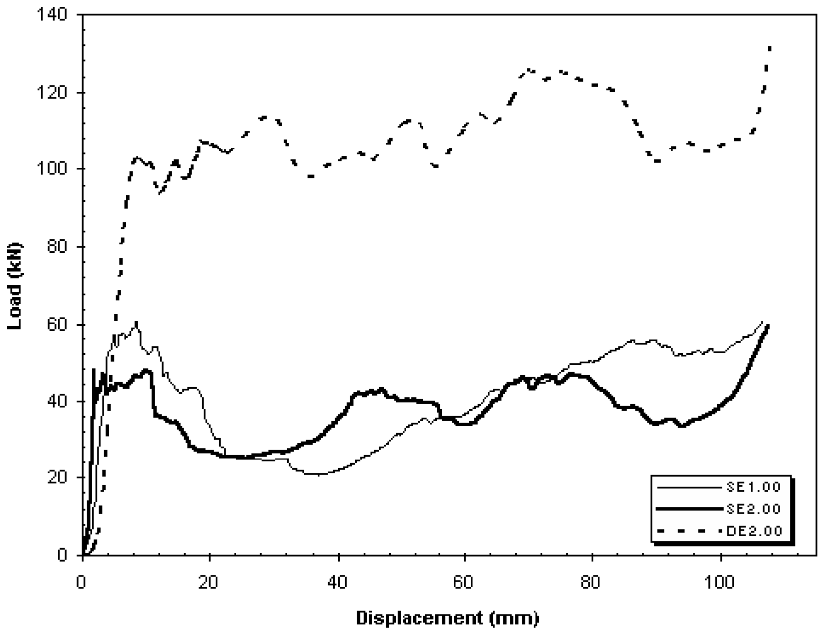

Figure 15. Typical load–deformation history of single and double elliptical tubes with core-less.

crushed portions remained intact. Moreover, the system significantly improved the space utilization compared with the core-less circular tube system and decreased the weight compared with the core-less single tube with the same ellipticity ratio. As shown in Fig. 15, this is brought about by establishment of a uniform sustained crushing load, high stroke efficiency and high specific energy absorption capability. Similar to core-less single system with ellipticity ratio of 2.00, pure regular progressive mode (Mode III) failure occurring from one end also dominates the crushing process of axially crushed core-less double elliptical tubes.

3.2. Specific energy absorption capability

The average energy absorbed as represented by the areas under the load–deflection curve is a function of specimen cross-sectional area, material density, and the crush distance:

$$E = \int P_{\mathrm{i}}\, \mathrm{d}s. \tag{1}$$

The integral is evaluated over the crushed distance. This will represent an approximation to the total work done in collapsing the structure, as the loading and displacement profiles in the other two mutually perpendicular directions are not considered. This is due to the fact that the work done can be defined as the force (P_{i}) multiplied by the displacement component in the direction of the force (ds). The integration required in equation (1) is replaced with a summation, as presented in equation (2), because there are a finite number of data points collected from the experimental test.

$$E = \sum_{i=1}^{N} P_{\mathrm{i}} \cdot \frac{(s_{i+1} - s_{i-1})}{2}. \tag{2}$$

The specific energy absorbed during the axial crushing of the tubes, which is equal to the area under the load–displacement curve, is evaluated as

$$E_{\mathrm{S}} = \frac{1}{M} \sum_{i=1}^{N-1} P_{\mathrm{i}} \cdot \frac{(s_{i+1} - s_{i-1})}{2} = \frac{1}{\rho \times A_1 h} \sum_{i=1}^{N-1} P_{\mathrm{i}} \cdot \frac{(s_{i+1} - s_{i-1})}{2} \tag{3}$$

in which A_1 is the material cross-section area, which can be calculated as $A_1 = \pi t(a + b + t)$. Moreover, to eliminate the effect of cross-section area on the energy absorbed, the specific energy absorption equation should be divided by the cross-section area of the structure to normalize the energy absorption as:

$$E_{\mathrm{NS}} = \frac{1}{\rho \times A_1^2 h} \sum_{i=1}^{N-1} P_{\mathrm{i}} \cdot \frac{(s_{i+1} - s_{i-1})}{2}. \tag{4}$$

3.3. Volumetric energy absorption capability

The volumetric energy absorption capability (i.e. energy absorbed per unit volume) is also an essential parameter for energy absorbing system design, where the space is a restraint factor. The volume occupied by composite elliptical tube before crushing can be calculated as $V = hA_2$, where, A_2 is the cross-sectional area occupied by the structure, given by $A_2 = \pi(a + t)(b + t)$. The energy absorbed per unit volume E_{V} can be calculated as

$$E_{\mathrm{V}} = \frac{E}{V} = \frac{1}{V} \sum_{i=1}^{N} P_{\mathrm{i}} \cdot \frac{(s_{i+1} - s_{i-1})}{2} = \frac{1}{\pi h(a + t)(b + t)} \sum_{i=1}^{N} P_{\mathrm{i}} \cdot \frac{(s_{i+1} - s_{i-1})}{2}. \tag{5}$$

Therefore, it could also be noted that the total energy absorbed (W_{T}) during the quasi-static axial crushing of core and core-less composite elliptical thin walled tubes is dissipated in two phases:

1. Energy absorbed during the pre-initial-crush failure phase (W_{picf}) is given by

$$W_{picf} = W_{mc} + W_{fd} + W_{bf} + W_{ff} + W_{del}, \tag{6}$$

   where W_{mc} is the energy required to crack the epoxy matrix; W_{fd} is the energy required to debond the woven roving fabric fibre from the matrix; W_{bf} is the energy required to buckle the longitudinal (0°) woven roving fabric fibre at crushed zone; W_{ff} is the energy required to fracture the hoop (90°) woven roving fabric fibre at crushed zone and W_{del} is the delamination energy or ply separation.

2. Energy absorbed during the post-crush failure phase (W_{pcf}) is given by

$$W_{pcf} = W_{ci} + W_{lc} + W_{sf} + W_{pof} + W_{ppof}, \tag{7}$$

where W_{ci} is energy required to deform the tube wall in circumferential direction; W_{lc} is the energy required for initiating a longitudinal shear cracking that in turn resulted in forming lamina bundles; W_{sf} is the energy required for splitting the formed lamina bundles from the structure; W_{pof} is the energy required for pulling out fibre and tearing the tube wall and W_{ppof} is the energy required for propagating crack down towards the bottom end of the core-tube.

Investigation using optical microscope has been carried out to explain the micro-failure mechanism as shown in Fig. 20.

3.4. Effect of ellipticity ratio on crushing behaviour

In order to study the effects of a/b ratio on the crashworthiness of composite elliptical tubes, the instantaneous load is normalized with respect to the cross-sectional area of the tube. Crush stresses were chosen to eliminate the influence of different cross-sectional areas so that the effect of ellipticity ratio remained. Table 1 lists the computed crashworthiness parameters. It is clearly seen that the load carrying capacity at post-crush failure stage is highly sensitive to the ellipticity ratio a/b. For the ellipticity ratios investigated, no obvious or consistent trends were associated with the variation in crush stresses. In some instances, as the ellipticity ratio increases from 1 to 1.75, the average crush stress increases. Among the core-less specimens tested, double elliptical tubes have the highest average crush stress value of 79 MPa, while the tube with a/b ratio of 1.00 (i.e. circular tube) recorded the lowest average crush stress of 51 MPa. Different trends were observed for average crush stress. It is also evident that as the ellipticity ratio increases, the average crush stresses decrease.

3.5. Effect of ellipticity ratio on energy absorption capability

Figure 16 shows the normalized specific energy–deformation curves for the composite elliptical tubes with various ellipticity ratios. From the energy–deformation curve, the accumulative energy absorbed from the tube at any displacement can be obtained. It can be seen from the figure that all the tubes have a non-linear energy deformation relation and the energy increases with increasing displacement. At pre-initial crush failure load, no damage is visible; however, as the load-carrying capacity of the tube increases matrix cracking occurs. As the crush load is further increased, the density and extent of the matrix cracks progress such that interfacial debonding occurs leaving the fibres unsupported, more compliant, and less likely to fail by shearing. This, in turn, leads to delamination, then fibre breakage, and finally, degrading of the material properties at the crush zone. This also causes the interlaminar strength of the composite to decrease. As interlaminar strength decreases, interlaminar cracks form at lower loads, resulting in a reduction in the energy absorption capability. Among all types of tubes investigated, specimens with ellipticity ratio of 2.0 exhibited the highest normalized specific energy owing to the cross-sectional area (A_1). These were in comparison to those of composite

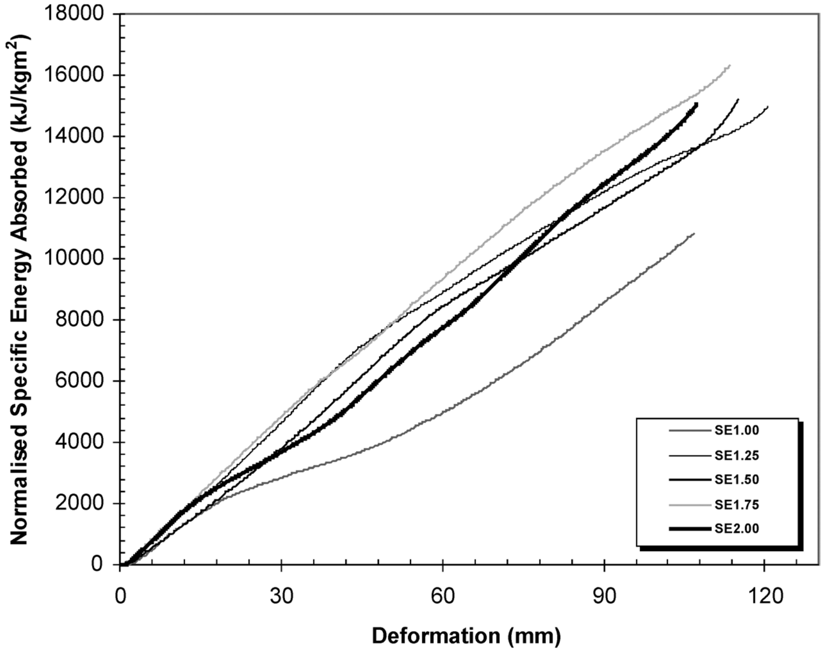

Figure 16. Normalized specific energy absorption–deformation curves of single composite elliptical tubes with core-less.

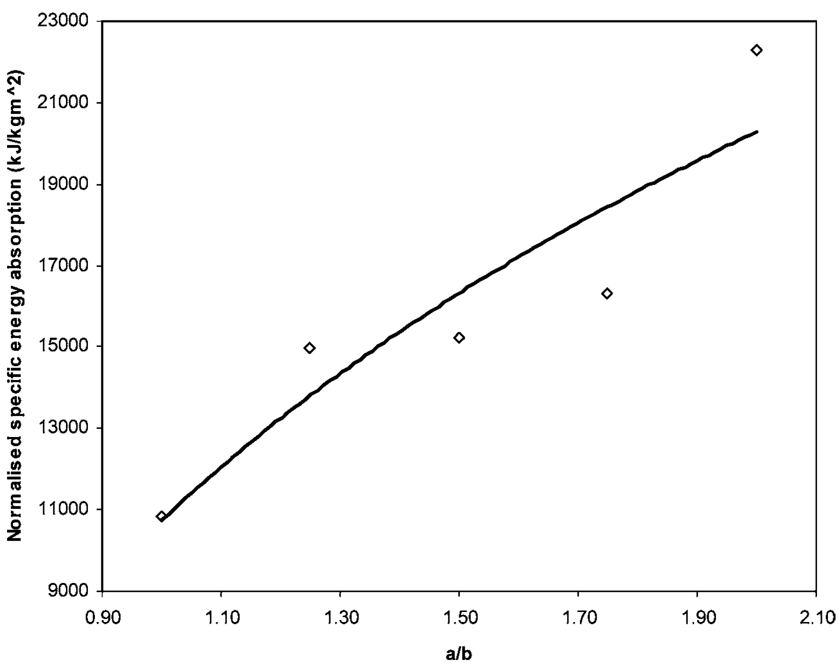

Figure 17. Variation of normalized specific energy absorption–deformation with ellipticity ratio.

circular tubes and other tubes with ellipticity ratios that varied between 1.5 and 2.0. The specimens with ellipticity ratio of 1.75 displayed the lowest energy absorption capability.

Figure 17 shows how the normalized specific energy absorbed varies with the ellipticity ratio a/b for core-less tubes. With increasing ratio (effectively decreasing major diameter), the specific energy absorbed increases in almost a logarithmic manner. The experimental data obtained fit the following empirical equation:

$$E_{\mathrm{NS}} = 1.38 \times 10^4 \ln(a/b) + 1.1 \times 10^4 \text{ kJ/kg m}^2. \tag{8}$$

3.6. Effect of tube arrangement

Normalized specific energy absorption–deformation curves for different arrangement system were shown in Fig. 18. It is evident that the double tubular system with ellipticity ratio of 2 absorbs significantly more energy than any of the other systems tested (nearly twice that of single core-less elliptical system with the same ellipticity ratio and over 2 times that of single core tubular system with ellipticity ratio of 1, i.e. circular tubes). In conclusion the double elliptical system demonstrates a lower peak force and a higher mean crush load, stable and higher crush loads during its large deformation process and a higher energy-absorption capability in terms of weight and space.

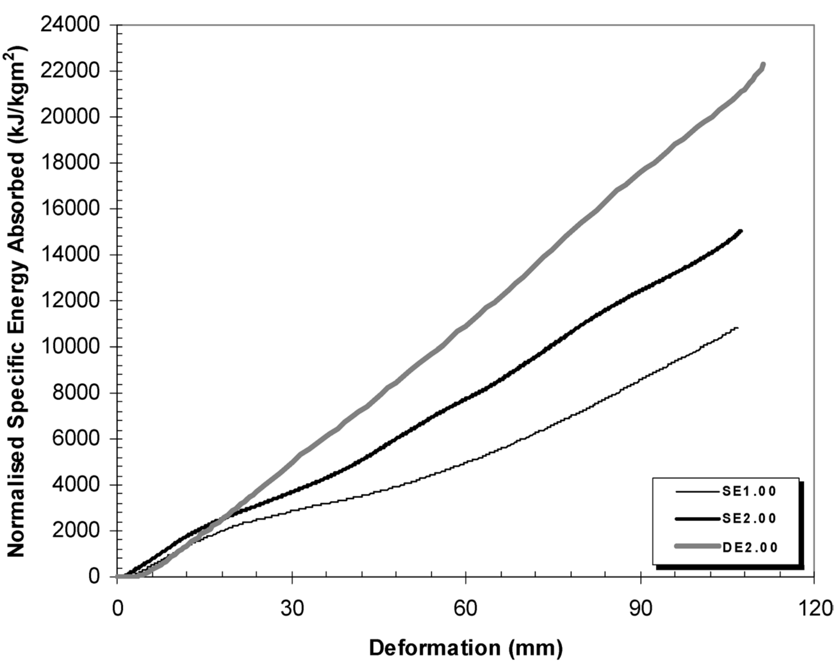

Figure 18. Normalized specific energy absorption–deformation curves of single and double elliptical tubes with empty cores.

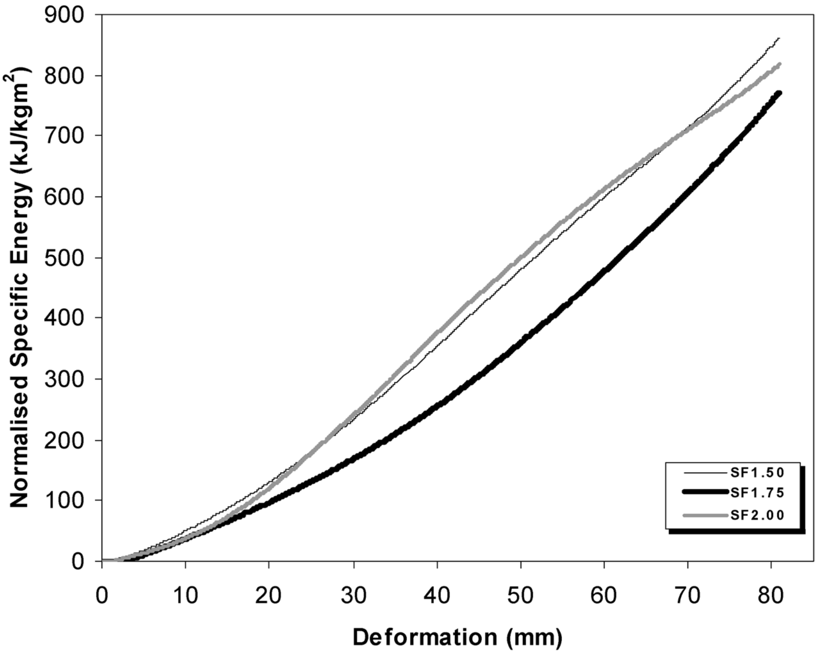

Figure 19. Normalized specific energy absorption–deformation curves of single composite elliptical tubes with core.

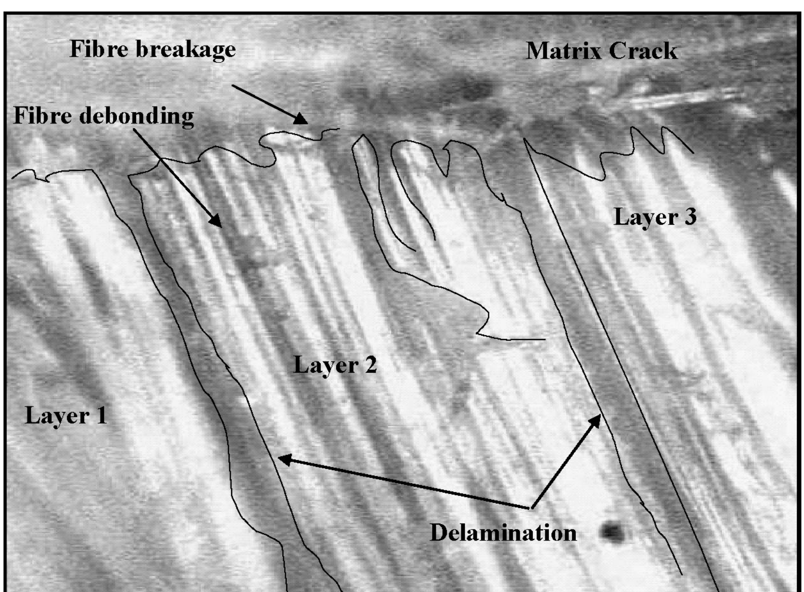

Figure 20. Failure mechanism at microscopic level (100 μm).

3.7. Effects of filling on load-carrying capacity

Experiments have revealed that natural fibre filling leads to a marked increase of the crushing force levels, as shown in Table 1. It is seen that the axial quasi-static crushing tests performed on cored single elliptical systems resulted in load carrying capacity significantly higher (nearly over 3 times) than the load carrying capacity obtained in tests with the core-less single elliptical systems. The most obvious factor that may affect this increase is that cored single elliptical systems have a larger presented cross-sectional area, so that they withstand very high crush loads before failing. This may be caused mainly by the activation of interaction effects, i.e. changes of the failure modes of the core-less tubes. Furthermore, the extensional stiffness matrix $\lfloor \boldsymbol{A}_{ij} \rfloor$ for these tubes is higher than the $\lfloor \boldsymbol{A}_{ij} \rfloor$ for the core-less tubes, which in turn increases significantly its membrane resistances.

3.8. Effects of filling on energy absorption capability

Normalized specific energy absorption–deformation curves for single core tube systems were shown in Fig. 19. The existence of filler leads to increases of the circumferential dissipation (owing to changed local or global buckling modes) of the tube wall. These effects also become obvious from the photos superimposed with the load–displacement curves in Figs 11–13. Within a moderate range of apparent mass density, natural fibre as filler material acts beneficially with respect to volumetric energy absorption of the whole crash element. Although the stroke efficiencies are reduced with natural fibre filling, marked increases of the volumetric energy absorption capacity are also observed for different test series. Compared to compression of cored and core-less tubes the increase of the volumetric energy absorption capability of core tubes is essentially affected by two mechanisms. On the one hand, the buckling of the tube wall is eliminated by the intrusion resistance of the core, causing a higher frequency of out-of-plane expansion and leading to an increase in the energy dissipation due to increased circumference deformations W_{ci}. On the other hand, the deformation capacity of the natural fibre core is exploited laterally by locally intrusion folds, leading to a multiaxial state of compression (and accordingly, higher energy dissipation) in the filler material.

4. CONCLUSION

Based upon the experimental and numerical results the following conclusions can be drawn:

1. The elastic energy absorbed is reduced considerably by implementing the double elliptical system arrangement and the presence of the natural fibre filler.
2. The intrusion resistance of the filler core shortens the buckling waves of the crushed zones.

3. The presence of the natural fibre filler increases significantly the tube crush load capacity.
4. The double elliptical system arrangement idealized the load–displacement curve.
5. If the total energy absorbed is the concern, the filled tubes have the highest energy absorption capability.
6. Considerable increase can be obtained for both the carrying capacity and the energy absorption capability by applying a cored double elliptical system arrangement.
7. The type of failure occurring was found to depend upon the magnitude of ellipticity ratio and the bending stiffness.
8. For the filled tubes, the high volumetric density of the structure results in a lower specific energy absorption capability.

It should be stated and bears repeating that utilizing the volume occupied by the shell collapsible energy absorber would be the best guides in developing an optimized energy absorbing system. This can only be achieved by using the idea of multi-system of energy absorber devices as obviously seen in the case of composite double elliptical tubes system.

Acknowledgements

The authors wish to thank University Putra Malaysia for the financial support for this research programme.

REFERENCES

1. D. Hull, Energy absorption of composite materials under crash conditions, in: *Progress in Science and Engineering of Composites, Proceedings of the 4th International Conference on Composite Materials (ICCM/4)*, Tokyo, pp. 861–870 (1982).
2. S. Ramakrishna and H. Hamada, Energy absorption characteristics of crash worthy structural composite materials, *Key Engineering Materials* **141-143**, 585–620 (1998).
3. W. Johnson and S. R. Reid, *Appl. Mech. Rev.* **31**, 277–288 (1978).
4. P. H. Thornton, Energy absorption in composite structure, *J. Compos. Mater.* **13**, 247–262 (1979).
5. T. Y. Reddy and S. T. S. Al-Hassani, Axial crushing of wood–filled square metal tubes, *Int. J. Mech. Sci.* **35** (3/4), 231–246 (1993).
6. M. F. Ashby, The mechanical properties of cellular solid, *MetalsTrans.* **14A**, 1755–1769 (1983).
7. L. J. Gibson and M. F. Ashby, *Cellular Solids*, 2nd edn. Cambridge University Press (1997).
8. P. H. Thornton, Energy absorption by foam filled structures, *SAE* Paper No. 800081 (1980).
9. E. Mahdi, B. B. Sahari, A. M. S. Hamouda and Y. A. Khalid, Effect of hybridisation on crushing behaviour of carbon/glass fibre/epoxy circular cylindrical shells, *J. Mater. Processing Technol.* **132** (1-3), 49–57 (2003).
10. D. Hui, Design of beneficial imperfection for elastic collapse of thin walled box columns, *Int. J. Mech. Sci.* **28**, 163–170 (1986).
11. A. S. Abosbaia, E. Mahdi, A. M. S. Hamouda and B. B. Sahari, Axial quasi-static crushing behaviour of segmented composite tubes, *Intern. J. Compos. Struct.* **60** (3), 327–343 (2003).

12. G. L. Farley, Effect of specimen geometry on the energy absorption capability of composite materials, *J. Compos. Mater.* **20**, 390–400 (1986).
13. G. L. Farley and R. M. Johnson, Analogy of the effect of material and geometrical variables on energy absorption capability of composite tubes, *J. Compos. Mater.* **26**, 78–90 (1992).
14. A. G. Mamalis, D. E. Manolakos, G. L. Viegelahn, S. M. Yap and G. A. Demosthenous, On the axial crumpling of fibre-reinforced composite thin-walled conical shells, *Intern. J. Vehicle Design* **12** (4), 450–467 (1991).
15. E. Mahdi, B. B. Sahari, A. M. S. Hamouda and Y. A. Khalid, Experimental quasi-static axial crushing of cone-tube-cone composite system, *Intern. J. Compos. Part B* **34** (3), 285–302 (2003).
16. L. Wu and J. F. Carney III, Initial collapse of braced elliptical tubes under lateral compression, *Int. J. Mech. Sci.* **39**, 1023–1036 (1997).
17. L. Wu and J. F. Carney III, Experimental analyses of collapse behaviours of braced elliptical tubes under lateral compression, *Int. J. Mech. Sci.* **40**, 761–777 (1998).
18. C. A. Meyres and M. W. Hyer, Response of composite elliptical cylinders to axial compression loading, *Mech. Compos. Mater. Structures* **6**, 169–194 (1999).
19. O. Alkolose, E. Mahdi and A. M. S. Hamouda, Axial crushing of composite elliptical tubes between flat platens, *Intern. J. Appl. Compos.* **10**, 6339–6363 (2003).
20. E. Mahdi, A. M. S. Hamouda, B. B. Sahari and Y. A. Khalid, Effect of reinforcement type and structure geometry on the crushing behaviour of circular conical glass fibre/epoxy, carbon fibre/epoxy and oil palm frond fibre/epoxy composite shells, *Intern. J. Appl. Compos.* **9** (5), 265–290 (2002).
21. S. R. Reid, T. Y. Reddy and M. D. Gray, Static and dynamic axial crushing of foam-filled sheet metal tubes, *Int. J. Mech. Sci.* **28** (5), 295–322 (1986).
22. W. Johnson and S. R. Reid, Metallic energy dissipating systems, *Applied Mechanics Reviews* **31**, 277–288 (1978). Update to this article in: *Applied Mechanics Reviews*, **39**, 303–319 (1986).
23. S. R. Reid, Plastic deformation mechanisms in axially compressed metal tubes used as impact energy absorbers, *Int. J. Mech. Sci.* **35** (12), 1035–1052 (1993).